

AN ANALYTICAL STUDY OF THE THERMALLY INDUCED TWO-PHASE FLOW INSTABILITIES INCLUDING THE EFFECT OF THERMAL NON-EQUILIBRIUM

P. SAHA* and N. ZUBER†

School of Mechanical Engineering, Georgia Institute of Technology, Atlanta, GA, U.S.A.

(Received 29 December 1976 and in revised form 21 July 1977)

Abstract—The problem of thermally induced flow instabilities in a uniformly heated boiling channel has been studied analytically. The effect of thermal non-equilibrium between the phases has been included by deriving a constitutive equation for the mass rate of vapor generation from steady state energy consideration. The system characteristic equation is derived by introducing a small perturbation in the inlet velocity, and the system stability boundary is determined by using the D -partition method. When compared with the equilibrium theory, the present non-equilibrium theory predicts a more stable system at low subcooling number and a more unstable system at high subcooling number. When compared with experiment, the present non-equilibrium theory agrees well with the data on the system stability boundary at low subcooling and the frequency of oscillations. However, further studies are required for better prediction of the system stability at high subcooling.

NOMENCLATURE

A_c , cross-sectional area of the channel [m^2];
 C_k , kinematic wave velocity [$m s^{-1}$];
 c_p , specific heat [$J kg^{-1} ^\circ C^{-1}$];
 D_i , coefficients in the characteristic equation (63);
 D_h , hydraulic diameter [m];
 $E(Z)$, function defined by equation (52);
 f , frequency of oscillation [Hz];
 f_f , liquid friction factor;
 f_m , mixture friction factor;
 G , mass velocity [$kg m^{-2} s^{-1}$];
 g , acceleration due to gravity [$m s^{-2}$];
 $H(Z, s)$, function defined by equation (53);
 i , specific enthalpy [$J kg^{-1}$];
 i_{fs} , saturated liquid enthalpy [$J kg^{-1}$];
 i_1 , enthalpy at the inlet of the channel [$J kg^{-1}$];
 Δi_{fg} , latent heat of vaporization, $i_g - i_{fs}$ [$J kg^{-1}$];
 Δi_{sub} , inlet subcooling, $i_{fs} - i_1$ [$J kg^{-1}$];
 Δi_z , subcooling at the point of net vapor generation, $i_{fs} - i_z$ [$J kg^{-1}$];
 j , volumetric flux density [$m s^{-1}$];
 k , thermal conductivity [$W m^{-1} ^\circ C^{-1}$];
 k_i, k_e , inlet and exit orifice coefficients, $\Delta P/\rho v^2$;
 l , length of the channel [m];
 Δl , characteristic length, $\lambda_{eq} - \lambda$ [m];

Δl_c , the length $\lambda_{CD} - \lambda$ defined in Fig. 3 [m];
 l_c^* , the ratio $\Delta l_c/\Delta l$;
 $N_{pch,eq}$, equilibrium phase change number, $\Omega_{eq} l/v_{fi}$;
 N_{sub} , subcooling number, $(\Delta \rho/\rho_g)(\Delta i_{sub}/\Delta i_{fg})$;
 P , pressure, bar ($1 \text{ bar} = 10^5 \text{ N m}^{-2}$);
 P_s , system pressure [bar];
 ΔP , pressure drop [bar];
 Pe , liquid Peclet number, $(\rho_f v_{fi} D_h c_{p,f})/k_f$;
 $Q(s)$, characteristic function;
 \dot{q}_w'' , wall heat flux [$W m^{-2}$];
 Re_{fs} , flow Reynolds number, $\rho_f v_{fi} D_h/\mu_f$;
 s , perturbation variable, $a + j\omega$, $[j = \sqrt{(-1)}]$;
 T , temperature [$^\circ C$];
 T_{sat} , saturation temperature [$^\circ C$];
 t , time [s];
 v , velocity [$m s^{-1}$];
 v_{fi} , velocity at the inlet of the channel [$m s^{-1}$];
 V_{gj} , vapor drift velocity, $v_g - j$ [$m s^{-1}$];
 x , actual vapor flow quality;
 x_{eq} , equilibrium vapor flow quality;
 $x_{e,eq}$, x_{eq} at the exit of the channel;
 Z , axial coordinate [m].

Greek symbols

α , vapor void fraction;
 Γ_g , mass rate of vapor generation per unit volume [$kg m^{-3} s^{-1}$];
 $\Gamma_{g,eq}$, Γ_g under thermal equilibrium assumption [$kg m^{-3} s^{-1}$];

* Present address: Department of Nuclear Energy, Brookhaven National Laboratory, Upton, NY 11973, U.S.A.

† Present address: Reactor Safety Research, U.S. Nuclear Regulatory Comm., Washington, D.C., U.S.A.

- ε , perturbation magnitude ($\ll \bar{v}_{fi}$)
 $[\text{m s}^{-1}]$;
 λ , distance of the boiling boundary from the inlet $[\text{m}]$;
 λ_{eq} , λ under thermal equilibrium assumption $[\text{m}]$;
 Λ_i , various transfer functions;
 μ , dynamic viscosity $[\text{kg m}^{-1} \text{s}^{-1}]$;
 ξ_h , heated perimeter $[\text{m}]$;
 ρ , density $[\text{kg m}^{-3}]$;
 $\Delta\rho$, density difference between the phases, $\rho_f - \rho_g$ $[\text{kg m}^{-3}]$;
 σ , surface tension $[\text{N m}^{-1}]$;
 τ_{12} , residence time in the heated liquid region $[\text{s}]$;
 τ_{34} , residence time in the region D defined in Fig. 3 $[\text{s}]$;
 Ω , local characteristic frequency of phase change $[\text{rad s}^{-1}]$;
 Ω_{eq} , equilibrium frequency of phase change, $\Gamma_{g,eq} \Delta\rho / (\rho_g \rho_f)$ $[\text{rad s}^{-1}]$;
 ω , angular frequency of oscillation $[\text{rad s}^{-1}]$.

Subscripts

- e , at the exit of the channel;
 ex , external;
 f , liquid phase;
 g , vapor phase (saturated);
 i or l , at the inlet of the channel;
 m , two phase mixture;
 s , saturation condition;
 w , at the wall;
 12 , heated liquid region;
 24 , heated mixture region;
 34 , region D defined in Fig. 3;
 λ , at the point of net vapor generation.

Superscripts

- $*$, [dimensionless].

Special notations

- \bar{G} , steady-state part of variable G ;
 δG , perturbed part of variable G .

1. INTRODUCTION

It is well known that thermally induced two-phase flow instabilities can introduce operational problems to steam generators, space propulsion systems, evaporators and various chemical process units. To avoid the occurrence of these undesirable events, it is essential to be able to predict accurately the onset of flow instabilities (i.e. flow oscillations and/or excursions) in such systems in terms of design parameters and operating conditions.

Of all the various types of two-phase flow instabilities, the low frequency oscillations, i.e. the so-called density wave oscillations, are the most common type encountered in practical systems [1]. As a result, this particular type of instability has been studied extensively during the last twenty years [2–14]. In all

the previous investigations, including the recent studies of Ishii and Zuber [12, 13] and Lahey and Yadigaroglu [14], the effect of thermal non-equilibrium between the phases, i.e. the local bulk temperature differences between the two phases, has been neglected. In reality, however, there are many instances where two phases can exist simultaneously even though their local bulk temperatures are different. One of the most common examples is the subcooled boiling region in a heated boiling channel where significant vapor generation can occur even though the local bulk temperature of the liquid is lower than the corresponding saturation temperature (or, the local vapor bulk temperature). This in effect, increases the length of the region occupied by the mixture; and at the same time, reduces the local rate of vapor generation in the mixture region because part of the heat added is utilized to increase the bulk temperature of the liquid. It is, therefore, impossible to predict the effect of thermal non-equilibrium on the stability of a system unless it is included in the dynamic analysis of the system.

The purpose of the present paper is, therefore, to include the effect of thermal non-equilibrium between the phases in the stability analysis of a heated boiling channel and compare the new analysis with the thermal equilibrium theory, and with the latest experimental data reported in [16 and 17].

2. EFFECT OF THERMAL NON-EQUILIBRIUM ON THE RATE OF VAPOR GENERATION

The vapor void fraction as well as the liquid bulk temperature along the length of a uniformly heated boiling channel is shown in Fig. 1. Liquid enters the

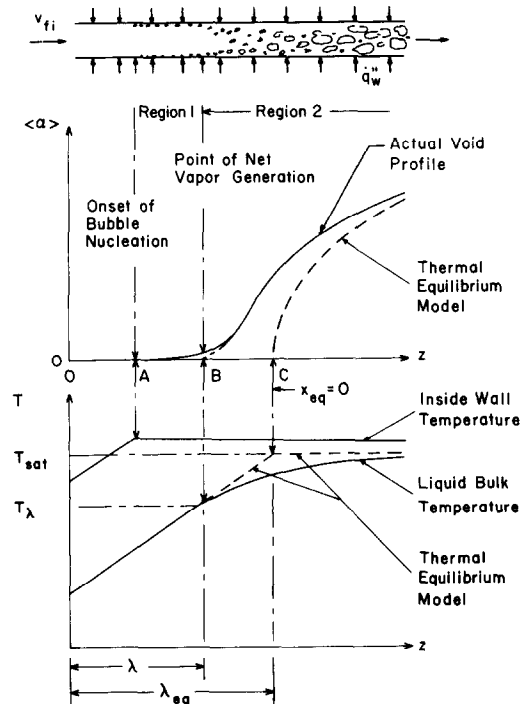


FIG. 1. A typical boiling channel.

channel at a temperature below the corresponding saturation temperature. Because of uniform heat flux distribution, the liquid bulk temperature starts to increase linearly. This would increase linearly up to the saturation value if all the heat added to the system would go to raise the temperature of the liquid only. After that, the liquid bulk temperature would remain constant at the saturation value and all the heat added would go to generate vapor. This is the thermal equilibrium model and is shown by the dotted lines in Fig. 1. Therefore, according to the equilibrium model, vapor generation starts from point C.

In reality, however, bubble generation starts at point A. At this point, the liquid bulk temperature is very much below the saturation temperature, i.e. the local subcooling is very high. However, the wall temperature is above saturation so that a thin superheated liquid film exists next to the wall. It is in this thin layer that the bubbles nucleate, grow, and eventually collapse after they penetrate into the subcooled liquid region. Therefore, the vapor void fraction cannot increase significantly until a point B is reached where the subcooling is low and the bubbles can move to the core of the flow. This point B, where the void fraction starts to increase rapidly, is considered as the initial point of net vapor generation. A correlation for this point has already been developed by the present authors [15, 16] which shows that for low mass-flow rates ($Pe < 70\,000$) the point of net vapor generation is thermally controlled, whereas for high mass-flow rates ($Pe > 70\,000$) it is governed by the fluid-dynamic conditions. As shown in Fig. 1, the liquid bulk temperature beyond this point is lower than that predicted by the thermal equilibrium model because a part of the heat added to the system is used to generate vapor. Therefore, a constitutive relation for the rate of vapor generation beyond point B is now required.

3. CONSTITUTIVE RELATION FOR THE RATE OF VAPOR GENERATION

For a two-phase mixture, the constitutive equation for the rate of vapor generation depends not only on the mode of heat transfer, but also on the topology of the liquid-vapor interface, i.e. the flow regime. Although a formal approach to determine this vapor generation rate in a bubbly flow has been proposed by Zuber *et al.* [18–20], its usefulness is restricted at this time due to uncertainties in determining the heterogeneous bubble nucleation rate and the subsequent bubble growth law.

An alternative approach is to make a realistic assumption about the liquid bulk enthalpy, i_f , and then determine the rate of vapor generation from the mixture energy equation. Neglecting the effects of kinetic and potential energy, and assuming a constant vapor phase enthalpy (equal to the corresponding saturation value), the steady-state mixture energy equation can be written as [18, 20]:

$$G(1-x)\frac{di_f}{dZ} + \Gamma_g(i_g - i_f) = \frac{\dot{q}_w \zeta_h}{A_c} \quad (1)$$

At the beginning of void formation, where $di_f(Z)/dZ$ is large, the value of actual quality, x , is much less than unity; subsequently, as x increases, $di_f(Z)/dZ \rightarrow 0$. Therefore, one can introduce the following simplification without much error:

$$(1-x)\frac{di_f(Z)}{dZ} \approx \frac{di_f(Z)}{dZ} \quad (2)$$

Since the subcooling at the point of net vapor generation, Δi_z , is usually much smaller than Δi_{fg} , one can also introduce that:

$$\Delta i_{fg} + (i_{fs} - i_f) \approx \Delta i_{fg} \quad (3)$$

In view of the above simplifications, which were first introduced by Ahmad [21], equation (1), can now be written as:

$$\Gamma_g(Z) = \frac{\dot{q}_w \zeta_h}{A_c \Delta i_{fg}} - \frac{G}{\Delta i_{fg}} \frac{di_f(Z)}{dZ} \quad (4)$$

Zuber *et al.* [18, 20] suggested the following liquid enthalpy distribution that satisfies the boundary conditions at $Z = \lambda$ and $Z \rightarrow \infty$:

$$\frac{i_f(Z) - i_z}{i_{fs} - i_z} = 1 - \exp\left(-\frac{Z - \lambda}{\Delta l}\right) \quad (5)$$

where the characteristic length Δl , is given by:

$$\Delta l = \lambda_{eq} - \lambda = \frac{GA_c(i_{fs} - i_z)}{\dot{q}_w \zeta_h} \quad (6)$$

With the above liquid enthalpy distribution, equation (4), i.e. the expression for the mass rate of vapor generation per unit volume, can be written as:

$$\Gamma_g(Z) = \frac{\dot{q}_w \zeta_h}{A_c \Delta i_{fg}} \left[1 - \exp\left(-\frac{Z - \lambda}{\Delta l}\right) \right] \quad (7)$$

For thermal equilibrium model, the liquid enthalpy in the two-phase mixture region is equal to i_{fs} and di_f/dZ is equal to zero. Therefore, from equation (1), the mass rate of vapor generation per unit volume under the thermal equilibrium assumption is:

$$\Gamma_{g,eq} = \frac{\dot{q}_w \zeta_h}{A_c \Delta i_{fg}} \quad (8)$$

Therefore, equation (7) can be written as:

$$\Gamma_g(Z) = \Gamma_{g,eq} \left[1 - \exp\left(-\frac{Z - \lambda}{\Delta l}\right) \right] \quad (9)$$

Recently, Lubbers [22] postulated a constitutive relation for the mass rate of vapor formation in the thermal non-equilibrium region similar to the first order reaction rate used in chemically reacting systems. For homogeneous flow, his constitutive relation yields the same equation as equation (9) for both steady-state and transient situations.

4. FORMULATION OF THE PROBLEM

Mathematical representation of a heated boiling channel with a large bypass is shown in Fig. 2. The components at the upstream of the inlet of the heated channel are lumped together and considered as an inlet

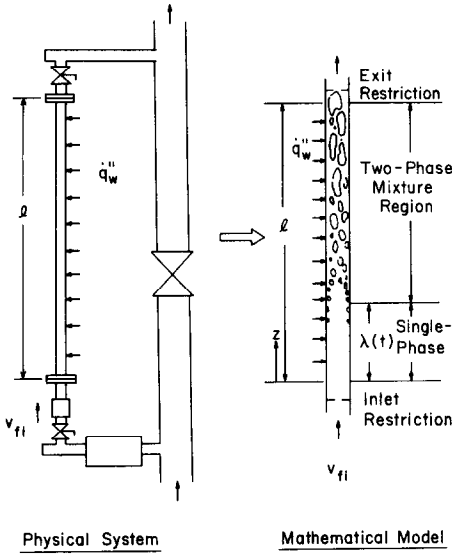


FIG. 2. Mathematical representation of the physical system.

restriction with orifice coefficient k_i . Similarly, the components at the downstream of the exit of the heated channel are considered as an exit restriction with orifice coefficient k_e . The length of the boiling channel is l and significant vapor generation starts at a distance λ from the inlet. The large unheated bypass imposes a constant pressure drop boundary condition across the boiling channel, which results from the steady-state flow rate, at the onset of flow instabilities. This is the same as having a flat pump characteristic, i.e.

$$\frac{\partial \Delta P_{ex}}{\partial v_{fi}} = 0. \quad (10)$$

4.1. Single-phase liquid region

The liquid is considered to be incompressible with constant thermodynamic and transport properties. Therefore, the conservation equations are:

1. Continuity.

$$\frac{\partial v_f}{\partial Z} = 0. \quad (11)$$

2. Momentum.

$$-\frac{\partial P}{\partial Z} = \rho_f \left(\frac{\partial v_f}{\partial t} + v_f \frac{\partial v_f}{\partial Z} \right) + \frac{f_f}{2D_h} \rho_f v_f^2 + g \rho_f. \quad (12)$$

3. Energy.

$$\frac{\partial i_f}{\partial t} + v_f \frac{\partial i_f}{\partial Z} = \frac{q''_w \zeta_h}{\rho_f A_c}. \quad (13)$$

As the liquid density, ρ_f , is a constant, the variables v_f , i_f , and P can be determined from the above conservation equations if the heat flux q''_w , and the single-phase liquid friction factor, f_f , are specified.

4.2. Two-phase mixture region

The mixture model or the drift-flux model is used to formulate the problem in the two-phase mixture

region. The time-smoothed, one-dimensional conservation equations as derived by Zuber and Ishii [11–13] are:

1. Conservation of mass of the mixture.

$$\frac{\partial \rho_m}{\partial t} + \frac{\partial}{\partial Z} (\rho_m v_m) = 0. \quad (14)$$

2. Conservation of mass of the vapor phase.

$$\frac{\partial}{\partial t} (\alpha \rho_g) + \frac{\partial}{\partial Z} (\alpha \rho_g v_g) = \Gamma_g. \quad (15)$$

3. Conservation of momentum of the mixture (neglecting the effect of surface tension).

$$\rho_m \left(\frac{\partial v_m}{\partial t} + v_m \frac{\partial v_m}{\partial Z} \right) = -\frac{\partial P_m}{\partial Z} - \frac{f_m}{2D_h} \rho_m v_m^2 - g \rho_m - \frac{\partial}{\partial Z} \left(\frac{\rho_f - \rho_m}{\rho_m - \rho_g} \frac{\rho_f \rho_g}{\rho_m} V_{gj}^2 \right). \quad (16)$$

4. Conservation of energy of the mixture (neglecting the effect of kinetic and potential energy).

$$\rho_m \left(\frac{\partial i_m}{\partial t} + v_m \frac{\partial i_m}{\partial Z} \right) = \frac{q''_w \zeta_h}{A_c} + \frac{\partial P_m}{\partial t} - \frac{\partial}{\partial Z} \left[\frac{\rho_f - \rho_m}{\rho_m} \frac{\rho_f \rho_g}{\Delta \rho} V_{gj} (i_g - i_f) \right]. \quad (17)$$

The mixture density, ρ_m , the mixture pressure, P_m , the mixture velocity, v_m , and the mixture enthalpy, i_m , are defined as:

$$\rho_m = \alpha \rho_g + (1 - \alpha) \rho_f \quad (18)$$

$$P_m = \alpha P_g + (1 - \alpha) P_f \quad (19)$$

$$v_m = \left(\frac{\alpha \rho_g}{\rho_m} \right) v_g + \left[\frac{(1 - \alpha) \rho_f}{\rho_m} \right] v_f \quad (20)$$

$$i_m = \left(\frac{\alpha \rho_g}{\rho_m} \right) i_g + \left[\frac{(1 - \alpha) \rho_f}{\rho_m} \right] i_f. \quad (21)$$

It should be noted that v_m and i_m represent the velocity and the enthalpy of the center of mass of the mixture, respectively.

The relative velocity between the phases is taken into account by introducing the vapor drift velocity, V_{gj} :

$$V_{gj} = v_g - j = (1 - \alpha)(v_g - v_f) \quad (22)$$

where, j , the volumetric flux density or the velocity of the center of volume of the mixture is given by:

$$j = \alpha v_g + (1 - \alpha) v_f. \quad (23)$$

Before trying to solve the problem in a general form, the following simplifying assumptions are introduced:

1. At any particular time and location, there is no pressure difference between the phases, i.e.

$$P_g = P_f = P. \quad (24)$$

Therefore,

$$P_m = \alpha P + (1 - \alpha) P = P. \quad (25)$$

2. The pressure drop across the channel is small compared to the system pressure or the inlet pressure. Therefore, the saturation temperature can be considered to be a constant throughout the length of the channel.

3. The enthalpy of the vapor phase is a constant and is equal to the corresponding saturation value.

4. Because of the constant vapor phase enthalpy and the small system pressure drop, the vapor phase density is assumed to be a constant. The liquid phase density has already been taken as a constant. Therefore, the mixture density, ρ_m , is a function of vapor void fraction only, i.e.

$$\rho_m = \rho_m(x). \quad (26)$$

It can be seen from equations (14)–(17) that the two continuity equations are written in Eulerian form, whereas the momentum and energy equations are in Lagrangian form. For convenience of solution, it is preferable to transform the continuity equations to the Lagrangian form. From equations (14) and (15) one can finally obtain [16]:

Equation for volumetric flux density:

$$\frac{\partial j}{\partial Z} = \frac{\Gamma_g \Delta \rho}{\rho_f \rho_g} \quad (27)$$

and, density propagation equation:

$$\frac{\partial \rho_m}{\partial t} + C_k \frac{\partial \rho_m}{\partial Z} = -\rho_m \frac{\Gamma_g \Delta \rho}{\rho_f \rho_g} \quad (28)$$

where, the kinematic wave velocity, C_k , is given by:

$$C_k = j + V_{gj} + \alpha \frac{\partial V_{gj}}{\partial \alpha}. \quad (29)$$

Discussion on kinematic (or continuity) wave may be found in [24, 25]. For bubbly-churn and slug flow, V_{gj} is independent of α [23]. For other flow regimes, such as annular or mist flow, it is assumed that

$$\alpha \frac{\partial V_{gj}}{\partial \alpha} \ll (j + V_{gj}). \quad (30)$$

Therefore, the density propagation equation (28) can be written as:

$$\frac{\partial \rho_m}{\partial t} + (j + V_{gj}) \frac{\partial \rho_m}{\partial Z} = -\rho_m \frac{\Gamma_g \Delta \rho}{\rho_f \rho_g}. \quad (31)$$

Since the phase densities are constant, the void fraction does not depend on the pressure drop in the channel. This implies that the mixture density, in the present analysis, is not a function of pressure. Therefore, one can solve for kinematics, i.e. the density and velocity field, of the flow first without considering the dynamics. It is apparent from equations (27) and (31) that if the vapor drift velocity, V_{gj} , and the mass rate of vapor generation per unit volume, Γ_g , are specified, one can solve for j and ρ_m . The mixture velocity, v_m , can then be determined from the identity:

$$v_m \equiv j - \left(\frac{\rho_f}{\rho_m} - 1 \right) V_{gj}. \quad (32)$$

In the previous section, a constitutive relation for the rate of vapor generation has been derived (equation 9). Recognizing that the boiling boundary, λ , is a function of time during flow instabilities, we modify equation (9) as:

$$\Gamma_g(Z, t) = \Gamma_{g,eq} \left[1 - \exp \left(- \frac{Z - \lambda(t)}{\Delta l} \right) \right] \quad (33)$$

where the characteristic length Δl still corresponds to the steady-state characteristic length ($\bar{\lambda}_{eq} - \bar{\lambda}$). Equation (33) is taken as the basic model for the rate of vapor generation in the solution that follows.

5. METHOD OF SOLUTION

Small perturbation technique, as already applied to several other instability analyses [5, 10–13], is used to linearize the system of governing equations. The disturbance is given in the form of an inlet velocity perturbation. Its responses to the boiling boundary, mixture density, mixture velocity and eventually to the channel pressure drop are determined. The inlet velocity is composed of a steady-state part and a perturbed part as given below:

$$v_{fi}(t) = \bar{v}_{fi} + \delta v_{fi}(t) = \bar{v}_{fi} + \varepsilon e^{st} \quad (34)$$

where $s = a + j\omega$; $j = \sqrt{-1}$.

In equation (34), s is a complex number; the real part a , is the amplification coefficient, whereas the imaginary part ω , represents the angular frequency of oscillation. It is assumed that ε/\bar{v}_{fi} is much smaller than unity and, therefore, only the first order term in ε is retained; the second and higher order terms are neglected.

6. SOLUTION

6.1. Boiling boundary

From the continuity equation for the single-phase liquid region, i.e. equation (11), the fluid velocity in the single-phase region is given by:

$$v_f = v_f(t) = v_{fi}(t) = \bar{v}_{fi} + \varepsilon e^{st}. \quad (35)$$

From the energy equation for the single-phase liquid region, i.e. equation (13), the boiling boundary between the single-phase liquid region and the two-phase mixture region can be given by:

$$\lambda(t) = \bar{v}_{fi} \tau_{12} + \varepsilon e^{st} \frac{(1 - e^{-s\tau_{12}})}{s} \quad (36)$$

where the residence time of a fluid particle in the single-phase region, τ_{12} , is:

$$\tau_{12} = \frac{\rho_f A_c (\bar{i}_\lambda - i_1)}{\dot{q}_w'' \zeta_h}. \quad (37)$$

If the local subcooling at the boiling boundary, i_λ , changes with a fluctuation in the inlet velocity, the residence time, τ_{12} , will also change. Therefore, in general,

$$\tau_{12} = \bar{\tau}_{12} + \delta \tau_{12} \quad (38)$$

where

$$\bar{\tau}_{12} = \frac{\rho_f A_c (\Delta i_{sub} - \bar{\Delta i}_\lambda)}{\dot{q}_w'' \zeta_h}. \quad (39)$$

The local subcooling at the boiling boundary, under the steady-state operation, is determined from [15, 16]:

$$\bar{\Delta i}_\lambda = i_{fs} - \bar{i}_\lambda = 0.0022 \frac{\dot{q}_w'' D_h c_{p,f}}{k_f}, \quad (Pe \leq 70\,000) \quad (40)$$

and

$$\bar{\Delta i}_\lambda = i_{fs} - \bar{i}_\lambda = 154 \frac{\dot{q}_w''}{\rho_f \bar{v}_{fi}}, \quad (Pe \geq 70\,000). \quad (41)$$

Defining

$$\Lambda_0 \equiv \frac{\partial \tau_{12}}{\partial v_{fi}} \quad (42)$$

one can write the transfer function for the perturbed part of the boiling boundary as:

$$\Lambda_1(s) \equiv \frac{\delta \lambda(t)}{\delta v_{fi}(t)} = \bar{v}_{fi} \Lambda_0 + \frac{(1 - e^{-s\tau_{12}})}{s}. \quad (43)$$

All the above expressions for the residence time and the boiling boundary make sense only if the inlet subcooling, Δi_{sub} , is greater than $\bar{\Delta i}_\lambda$. On the other hand, if the inlet subcooling, Δi_{sub} , is lower than $\bar{\Delta i}_\lambda$, it is assumed that boiling starts right from the inlet of the heated channel. In that case, one obtains:

$$\tau_{12} = 0 \quad \text{and} \quad \lambda(t) = 0 \quad (\Delta i_{sub} < \bar{\Delta i}_\lambda) \quad (44)$$

Consequently,

$$\bar{\tau}_{12} = 0 \quad \text{and} \quad \bar{\lambda} = 0 \quad (45)$$

and

$$\Lambda_0 = 0 \quad \text{and} \quad \Lambda_1(s) = 0. \quad (46)$$

6.2. Mixture density and velocity

Integrating equations (27) and (31), the final expressions for the steady-state and perturbed part of the mixture density are:

$$\frac{\bar{\rho}_m(Z)}{\rho_f} = \frac{\bar{C}_k(\bar{\lambda})}{\bar{C}_k(Z)} = \frac{\bar{v}_{fi} + \bar{V}_{gj}}{\bar{v}_{fi} + \bar{V}_{gj} + \int_{\lambda}^Z \bar{\Omega}(Z) dZ} \quad (47)$$

and

$$\begin{aligned} \frac{1}{\rho_f} \frac{\delta \rho_m(Z, t)}{\delta v_{fi}(t)} &\equiv \Lambda_4(Z, s) \\ &= \left[\frac{\bar{C}_k(\bar{\lambda})}{\bar{C}_k(Z)} \right] e^{-s[E(Z) - E(\bar{\lambda})]} \\ &\times \left[\frac{\bar{\Omega}(\bar{\lambda}) \Lambda_1(s)}{\bar{C}_k(\bar{\lambda})} + \{H(Z, s) - H(\bar{\lambda}, s)\} \right] \end{aligned} \quad (48)$$

where the characteristic frequency of phase change, $\Omega(Z, t)$, and the other terms are defined as:

$$\Omega(Z, t) = \Gamma_g(Z, t) \frac{\Delta \rho}{\rho_g \rho_f} = \bar{\Omega}(Z) + \delta \Omega(Z, t) \quad (49)$$

$$\Lambda_2(Z, s) \equiv \frac{\delta \Omega(Z, t)}{\delta v_{fi}(t)} \quad (50)$$

$$\Lambda_3(Z, s) \equiv \frac{\delta C_k(Z, t)}{\delta v_{fi}(t)} \quad (51)$$

$$E(Z) \equiv \int \frac{dZ}{\bar{C}_k(Z)} \quad (52)$$

and

$$\begin{aligned} H(Z, s) &\equiv \int e^{s[E(Z) - E(\bar{\lambda})]} \\ &\times \left\{ -\frac{\Lambda_2(Z, s)}{\bar{C}_k(Z)} + \frac{\Lambda_3(Z, s)}{[\bar{C}_k(Z)]^2} \frac{d\bar{C}_k(Z)}{dZ} \right\} dZ. \end{aligned} \quad (53)$$

It should be noticed that, in the thermal equilibrium model, the characteristic frequency of phase change is a constant, i.e. Ω_{eq} or $\Gamma_{g,eq}(\Delta \rho / \rho_f \rho_g)$. However, in the present non-equilibrium model, the characteristic frequency, $\Omega(Z, t)$, is not a constant; it consists of a spatially non-uniform steady part, $\bar{\Omega}(Z)$, and a perturbed part, $\delta \Omega(Z, t)$.

From identity (32), the steady-state and the perturbed part of the mixture velocity are given by:

$$\frac{\bar{v}_m(Z)}{\bar{v}_{fi}} = \frac{\bar{C}_k(Z)}{\bar{C}_k(\bar{\lambda})} = \frac{\rho_f}{\rho_m(Z)} \quad (54)$$

and

$$\begin{aligned} \frac{\delta v_m(Z, t)}{\delta v_{fi}(t)} &\equiv \Lambda_5(Z, s) \\ &= \Lambda_3(Z, s) + \left[\frac{\bar{C}_k(Z)}{\bar{C}_k(\bar{\lambda})} \right]^2 V_{gj} \Lambda_4(Z, s). \end{aligned} \quad (55)$$

6.3. System pressure drop and characteristic equation

Integrating the momentum equations, i.e. equations (12) and (16), and adding all the perturbed parts, one obtains the response of the system pressure drop to the inlet flow fluctuation as:

$$\begin{aligned} \frac{\delta \Delta P_s(t)}{\delta v_{fi}(t)} &\equiv Q(s) = 2k_i \rho_f \bar{v}_{fi} + \rho_f \left[s\bar{\lambda} + \frac{f_f}{D_h} \bar{v}_{fi} \bar{\lambda} \right] \\ &+ \Lambda_8(s) + \Lambda_9(s) + \Lambda_{10}(s) + \Lambda_{11}(s) \\ &+ \Lambda_{12}(s) + \Lambda_{13}(s) \end{aligned} \quad (56)$$

where, the transfer functions, $\Lambda_8(s)$ through $\Lambda_{13}(s)$ represent the various pressure drop responses, i.e. the local acceleration, convective acceleration, gravity, frictional, drift and exit restriction, in the two-phase mixture region.

In a practical system there is always some small fluctuation in the system pressure drop, and it is this fluctuation that causes a variation in the inlet flow. In terms of control theory, $\delta \Delta P_s$ is the generalized input force, δv_{fi} is the output displacement, and $1/Q(s)$ is the system transfer function. If all the roots of the characteristic equation

$$Q(s) = 0 \quad (57)$$

lie in the left half of the s -plane, every component of disturbance tends to zero as time approaches infinity. This is the necessary condition for asymptotic stability.

In view of the assumption of flat pump characteris-

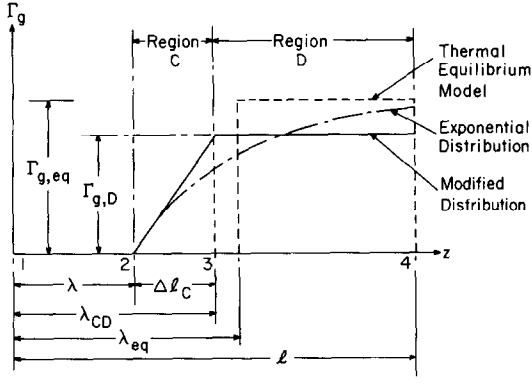


FIG. 3. Modified distribution for the rate of vapor generation.

tic, i.e. equation (10), the condition for excursive stability is:

$$\lim_{s \rightarrow 0} \frac{\delta \Delta P_s}{\delta v_{fi}} = \lim_{s \rightarrow 0} Q(s) > 0. \quad (58)$$

It can be seen from equation (56) that, to solve the instability problem, it is now necessary to be able to obtain analytical expressions for various transfer functions, namely $\Lambda_8(s)$ through $\Lambda_{13}(s)$. In spite of

The final form of the dimensionless characteristic equation is:

$$\begin{aligned} \frac{Q(s)}{(\rho_f \Omega_{eq} l) \bar{v}_{fi}^*} &\equiv Q^*(s^*) = \frac{1}{(s^*)^2 (s^* - l_c^*)^2 (s^* - 2l_c^*)} \\ &\times [(D_1 s^{*7} + D_2 s^{*6} + D_3 s^{*5} + D_4 s^{*4} + D_5 s^{*3} + D_6 s^{*2} + D_7 s^* + D_8) \\ &+ (D_9 s^{*6} + D_{10} s^{*5} + D_{11} s^{*4} + D_{12} s^{*3} + D_{13} s^{*2} + D_{14} s^* + D_{15}) e^{-s^* \tau_{t2}} \\ &+ (D_{16} s^{*6} + D_{17} s^{*5} + D_{18} s^{*4} + D_{19} s^{*3} + D_{20} s^{*2} + D_{21} s^* + D_{22}) e^{-s^* \tau_{t3}^4} \\ &+ (D_{23} s^{*5} + D_{24} s^{*4} + D_{25} s^{*3} + D_{26} s^{*2} + D_{27} s^* + D_{28}) e^{-s^* (\tau_{t2}^* + \tau_{t3}^*)}] \end{aligned} \quad (63)$$

concerted efforts, it was not possible to obtain analytical expressions for these transfer functions by using the exponential form of the rate of vapor generation, i.e. equation (33). Even the transfer function for the perturbation of mixture density, i.e. $\Lambda_4(Z, s)$, could not be determined analytically due to severe complexity involved in the integration defined by equation (53). Therefore, the two-phase mixture region is divided into two regions, as shown in Fig. 3. In the first region, i.e. region C, Γ_g increases linearly:

$$\Gamma_{g,C}(Z, t) = \Gamma_{g,eq} \left[\frac{Z - \lambda(t)}{\Delta l_c} \right] \quad (\lambda \leq Z \leq \lambda + \Delta l_c). \quad (59)$$

Note that the slope of the above distribution at the boiling boundary is the same as that of the exponential distribution. In the second region, i.e. region D, Γ_g remains constant:

$$\Gamma_{g,D} = \Gamma_{g,eq} \frac{\Delta l_c}{\Delta l}, \quad (\lambda + \Delta l_c \leq Z \leq l). \quad (60)$$

The boundary between the two regions, i.e. the distance Δl_c from the boiling boundary, is determined such that the steady-state exit vapor quality under the

present approximate model remains the same under the original exponential model. That is:

$$\begin{aligned} \int_{\lambda}^l \Gamma_g(Z) dZ \\ = \int_{\lambda}^{\lambda + \Delta l_c} \Gamma_{g,C}(Z) dZ + \int_{\lambda + \Delta l_c}^l \Gamma_{g,D} dZ. \end{aligned} \quad (61)$$

From the above equation, the physically realistic solution for Δl_c is:

$$\Delta l_c = (l - \lambda) - \left[(l - \lambda)^2 - 2\Delta l \left\{ (l - \lambda) - \Delta l \left[1 - \exp\left(-\frac{l - \lambda}{\Delta l}\right) \right] \right\} \right]^{1/2}. \quad (62)$$

The transfer functions $\Lambda_8(s)$ through $\Lambda_{13}(s)$ are then evaluated using a lumped parameter model for the two-phase friction factor, f_m . The expressions for these transfer functions are rather long, and could not be presented here due to space limitation. They can be found in [16].

The characteristic equation (56) is non-dimensionalized using the length of the channel, l , and the equilibrium reaction time, $1/\Omega_{eq}$, as the basic scaling parameter for length and time, respectively.

where

$$s^* = s/\Omega_{eq} \quad (64)$$

and

$$l_c^* = \Delta l_c/\Delta l. \quad (65)$$

The coefficients D_i are composed of another set of coefficients C_i presented in [16] which can be calculated from the system geometry and operating conditions.

6.4. Determination of stability boundary

The D -partition method [13, 26, 27] is used to determine the system stability boundary in the subcooling number vs the equilibrium phase change number plane introduced by Ishii and Zuber [12, 13]. The subcooling number, $(\Delta\rho/\rho_g)(\Delta i_{sub}/\Delta i_{fg})$, scales the inlet subcooling and is the dimensionless residence time of a fluid particle in the single-phase region under the thermal equilibrium assumption. The equilibrium phase change number, $\Omega_{eq} l/\bar{v}_{fi}$, scales the rate of phase change due to heat addition under the thermal equilibrium assumption and is similar to the Damköhler group I in chemical kinetics. Setting s^* equal to $j\omega^*$ in equation (63) and resolving it into real and imaginary parts, and setting both parts equal to zero, one can

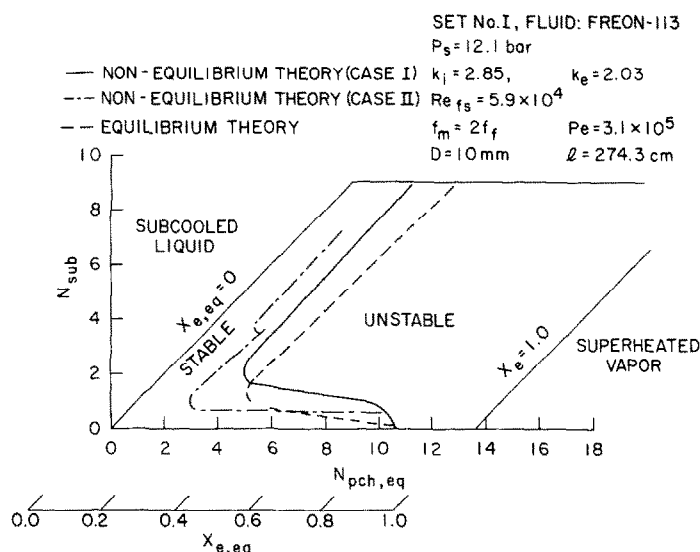


FIG. 4. Comparison between the equilibrium and the non-equilibrium theories.

eliminate the auxiliary parameter ω^* and find a relationship between the subcooling number, N_{sub} , and the equilibrium phase change number, $N_{pch,eq}$, holding k_i , k_e , Re_{fs} , etc. constant. The procedure results in the construction of neutral stability boundaries which divide the stability plane in several regions [16]. Stability of each of these regions is then determined by using the Mikhailov criterion or the Encirclement theorem [13, 26, 27]. The condition for excursive stability is checked by taking $\lim \omega^* \rightarrow 0$ in equation 63.

7. RESULTS AND DISCUSSIONS

From the correlation for determining the point of net vapor generation, i.e. equations (40) and (41), it can be seen that at least for steady-state operation, the local subcooling at the point of net vapor generation is inversely proportional to the inlet velocity for high mass fluxes ($Pe > 70,000$). Whether the same conclusion can be extended to a transient oscillatory flow problem depends on the magnitude of the characteristic Strouhal number, which is the ratio of the characteristic residence time of a fluid particle to the time period of oscillation. Therefore, two different cases have been examined for $Pe > 70,000$:

Case I: Assume that the local subcooling at the boiling boundary, in the transient analysis, does not change with inlet flow fluctuation, i.e. $\Lambda_0^* = 0$.

Case II: Assume that the local subcooling at the boiling boundary changes, even in the transient case, according to equation (41), i.e. $\Lambda_0^* = 154(A_c \Omega_{cu} / \zeta h f_h)$.

In Fig. 4, the stability boundaries for both Case I and Case II are shown for a typical input data. The vapor drift velocity corresponding to the upward bubbly-churn flow is used, and the mixture friction factor is taken to be twice the single-phase liquid friction factor. For Case I, the first neutral stability boundary is found to be the system stability boundary. For Case II, however, the second neutral stability

boundary overtakes the first one at a higher subcooling number and becomes the system stability boundary as shown in Fig. 4. It can also be seen that Case II predicts a more unstable system than Case I. This is due to the fact that, in Case II, the non-zero positive value of Λ_0^* adds to the fluctuation of the boiling boundary which has a destabilizing effect on the system.

In Fig. 4, the results of the non-equilibrium theory (both Cases I and II) are also compared with the equilibrium theory of Ishii and Zuber [13, 12]. For the case of zero inlet subcooling, the system is under thermal equilibrium. Therefore, the prediction of the non-equilibrium theory coincides with that of the equilibrium theory as expected. As the subcooling number increases, the non-equilibrium model starts to predict a more stable system because for $\Delta i_{sub} < \Delta i_j$, vapor generation still starts at the inlet of the heated channel which implies that there is no time delay in the single-phase region (in fact, there is no single-phase region at all). As the subcooling number increases beyond a certain value, the single-phase liquid region appears and the non-equilibrium model predicts a more unstable system. It can be noticed, however, that like the equilibrium model, the non-equilibrium stability boundary is also almost parallel to the constant equilibrium exit quality line at a high subcooling number.

In Fig. 5, the experimental data [16, 17] on the onset of flow oscillation corresponding to various system pressures (set Nos. I, II, and III) are compared with the present non-equilibrium theories (both Case I and Case II) as well as with the equilibrium theory of Ishii and Zuber [12, 13]. The effect of system pressure is well-absorbed by the non-dimensional co-ordinates, i.e. the subcooling number and the equilibrium phase change number. It can be seen from Fig. 5, that, except for high subcooling number, the non-equilibrium theory with $\Lambda_0^* = 0$, i.e. Case I, predicts results which are conservative but in closer agreement with the

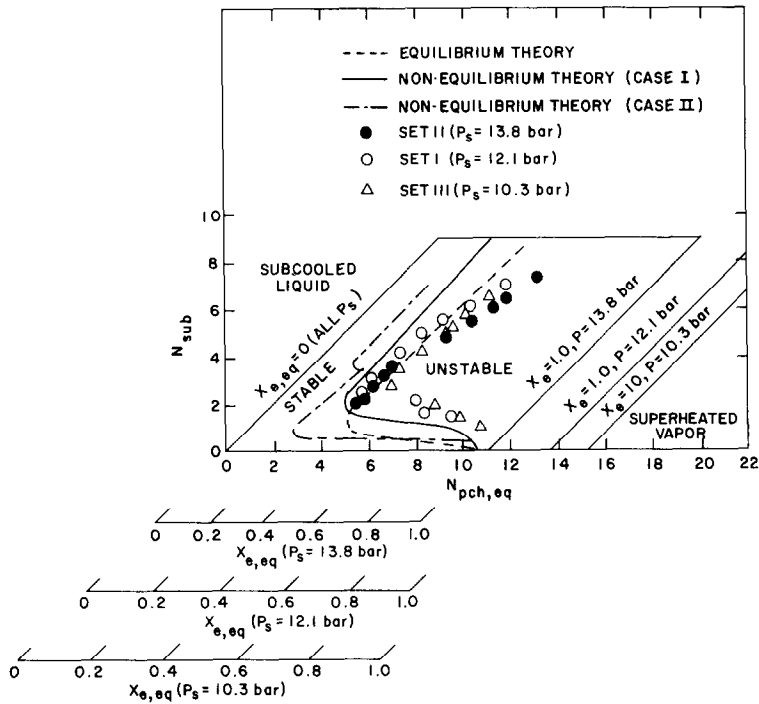


FIG. 5. Comparison of experimental data [16, 17] on the onset of flow oscillations with various theoretical predictions.

system stability boundary formed by the experimental data. The equilibrium theory of Ishii and Zuber is more conservative at low subcooling numbers and is non-conservative at moderate subcooling numbers. On the other hand, the non-equilibrium theory with $\Lambda_0^* = 154(A_c \Omega_{eq} / \xi_{if})$ i.e. Case II, is very conservative at every subcooling number.

The experimental data on the frequency of oscillations for the same sets of runs are compared with various theories in Fig. 6. It is clear that the non-equilibrium theory with $\Lambda_0^* = 0$, i.e. Case I, is the best. Moreover, a discontinuity is resulted in the prediction of Case II as the second neutral stability boundary becomes the system stability boundary at a certain subcooling number.

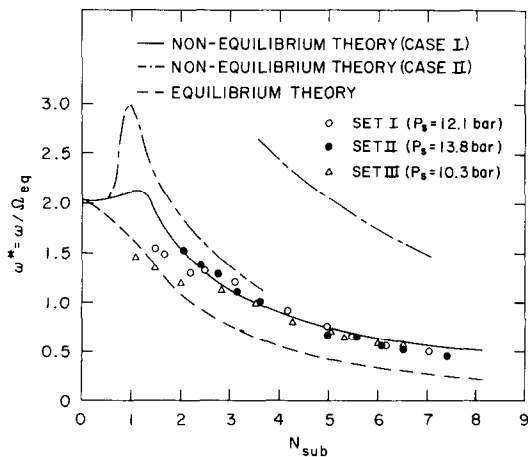


FIG. 6. Comparison of experimental data [16, 17] on the frequency of oscillation with various theoretical predictions.

To check the above findings further, another set of experimental data with larger inlet restriction (set number IV) is compared with the non-equilibrium as well as the equilibrium theories in Figs. 7 and 8. From these figures, it can be seen that the non-equilibrium theory with $\Lambda_0^* = 0$ is again the best choice for predicting the system stability boundary and the frequency of oscillation. This implies that in the present transient cases, it is more appropriate to assume that the local subcooling at the boiling boundary does not change due to a small perturbation in the inlet velocity. It is found from experiments that the time period of oscillation, τ_{os} , for the so-called density wave oscillations considered here, is indeed on the order of the characteristic residence time, l/\bar{v}_{fi} . As a result, the characteristic Strouhal number, $l/\bar{v}_{fi}\tau_{os}$, is on the order of unity. It is plausible that the characteristic Strouhal number has to be much smaller than unity before one can extend the conclusions derived from steady-state data to the non-steady oscillatory situations. In other words, the bubble dynamics at the boiling boundary may not be able to follow a quasi-steady-state behavior unless the time period of oscillation is very large compared to the characteristic residence time.

One common feature has been observed from the experimental data presented here and reported in [16, 17]. As the subcooling number is increased beyond a critical value, the stability boundary formed by the experimental data always bends towards the right hand side from a constant equilibrium exit quality line. This trend has also been observed in other experimental investigations (for example, see Solberg's steam-water data as presented in Fig. 4 of [12]). The

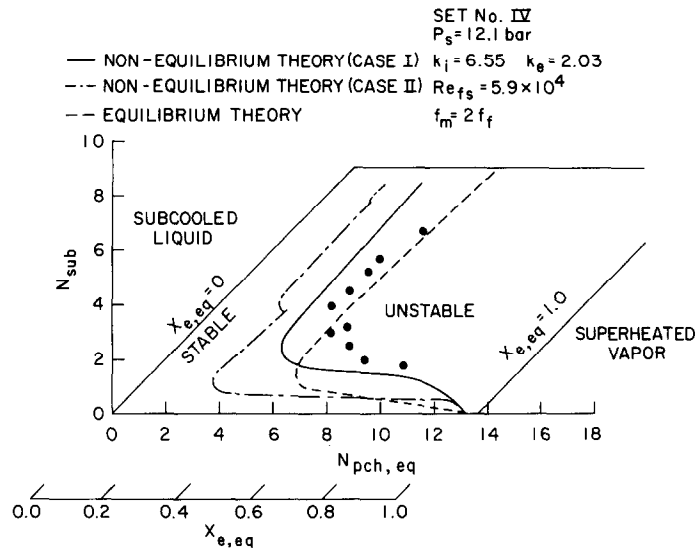


FIG. 7. Comparison of experimental data [16, 17] on the onset of flow oscillations with various theoretical predictions.

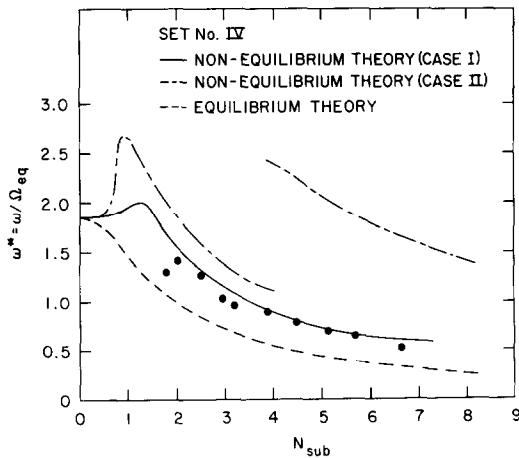


FIG. 8. Comparison of experimental data [16] on the frequency of oscillation with various theoretical predictions.

theoretical predictions, however, remain almost parallel to a constant equilibrium exit quality line, i.e. the onset of flow oscillation according to the theories take place at a characteristic equilibrium exit quality.

Several possible aspects were examined for this discrepancy. First, the two-phase friction factor is actually a function of vapor void fraction which increases along the length of the channel. In the present analysis, the mixture friction factor is taken to be a constant. However, according to the analysis of Ishii [13], the mixture friction factor has very little effect on the system stability boundary at high subcooling number.

Secondly, because of the one-dimensional treatment of the problem, the value of the void distribution parameter, C_0 [23], defined as $\langle \alpha j \rangle / (\langle \alpha \rangle \langle j \rangle)$, is implicitly equal to one. Furthermore, the vapor drift velocity for the bubbly-churn turbulent flow is used irrespective of the flow regime. In the actual system, however, the value of the void distribution parameter

is usually greater than one [15, 23], and in annular flow regime the relative velocity between the phases can be much higher than what is accounted for by using the drift velocity for bubbly flow. Both of these aspects of the actual system lead to a lower void fraction, i.e. a higher mixture density which has a stabilizing effect. Therefore, it appears that in addition to the effect of thermal non-equilibrium, one should use more realistic values of void distribution parameter and vapor drift velocity to be able to predict the actual system behavior more accurately.

8. CONCLUSIONS

A constitutive equation for the mass rate of vapor generation per unit volume has been derived for the thermal non-equilibrium region, i.e. the subcooled boiling region, from a logical choice of the liquid bulk enthalpy.

The effect of thermal non-equilibrium has been incorporated in the transient analysis of a heated boiling channel, and a system characteristic equation has been derived by using the small perturbation technique.

The system stability boundary including the effect of thermal non-equilibrium predicts a more stable system at low subcooling number, and more unstable system at high subcooling number when compared with the thermal equilibrium theory of Ishii and Zuber [12, 13].

Comparison of the latest experimental data on the onset of flow oscillation with various theories indicates that the present non-equilibrium theory (assuming no change in local subcooling at the boiling boundary) predicts the system stability boundary quite well at low subcooling. It also agrees well with the frequency of oscillation for a broad range of subcooling. However, further studies are needed for better prediction of the system stability boundary at high subcooling.

Acknowledgements—The study was sponsored by the National Science Foundation under grant number GK-16023, and it was carried out in the School of Mechanical Engineering, Georgia Institute of Technology, Atlanta, Georgia. Assistance rendered by Brookhaven National Laboratory and U.S. Nuclear Regulatory Commission in preparing the manuscript is also appreciated.

REFERENCES

1. J. A. Bouré, A. E. Bergles and L. S. Tong, Review of two-phase flow instability, ASME Paper No. 71-HT-42 (1971).
2. E. P. Serov, The operation of once-through boilers in variable regimes, *Trudy Mosk Energ. Inst.* **11** (1953).
3. E. P. Serov, Transient process in steam generators, *Teploenergetika* **13**(9), 50 (1966).
4. E. P. Serov, Analytical investigation of the boundary conditions for the formation of pulsation in steaming pipes during forced circulation, *High Temperature* **3**, 545 (1965).
5. G. B. Wallis and J. H. Heasley, Oscillation in two-phase flow system, *J. Heat Transfer* **83C**, 363 (1961).
6. J. Bouré, Instabilités hydrodynamiques limitant la puissance des réacteurs à eau bouillante, Final report EUR 2389 F, EURAEC 1464 (June 1965).
7. J. Bouré, The oscillatory behavior of heated channels. An analysis of density effects, C.E.A.R. 3049, Centre d'Etudes Nucleaires de Grenoble, France (1966).
8. J. Meyer and R. Rose, Application of a momentum integral model to the study of parallel channel boiling flow oscillations, *J. Heat Transfer* **85C**, 1 (1963).
9. M. B. Carver, An analytical model for the prediction of hydrodynamic instability in parallel heated channels, Report No. AECL-2681, Atomic Energy of Canada Ltd, Chalk River, Ontario (1967).
10. N. Zuber, An analysis of thermally induced flow oscillations in the near-critical and super-critical thermodynamic region, Final Report NAS8-11422, N.A.S.A. (1966).
11. N. Zuber, Flow excursions and oscillations in boiling two-phase flow systems with heat addition, in *Symposium on Two-Phase Flow Dynamics*, Eindhoven, Vol. 1, p. 1071. EURATOM, Brussels (September 1967).
12. M. Ishii and N. Zuber, Thermally induced flow instabilities in two-phase mixtures, Paper No. B5.11, in *Proceedings of the Fourth International Heat Transfer Conference*, Paris. Elsevier, Amsterdam (1970).
13. M. Ishii, Thermally induced flow instabilities in two-phase mixtures in thermal equilibrium, Ph.D. Thesis, School of Mechanical Engineering, Georgia Institute of Technology, Atlanta, Georgia (June 1971).
14. R. T. Lahey and G. Yadigaroglu, A Lagrangian analysis of two-phase hydrodynamics and nuclear-coupled density-wave oscillations, Paper No. B5.9, in *Proceedings of the Fifth International Heat Transfer Conference*, Tokyo, Japan, Vol. IV. JSME and SCEJ, Tokyo (1974).
15. P. Saha and N. Zuber, Point of net vapor generation and vapor void fraction in subcooled boiling, Paper No. B4.7, in *Proceedings of the Fifth International Heat Transfer Conference*, Tokyo, Japan, Vol. IV. JSME and SCEJ, Tokyo (1974).
16. P. Saha, Thermally induced two-phase flow instabilities, including the effect of thermal non-equilibrium between the phases, Ph.D. Thesis, School of Mechanical Engineering, Georgia Institute of Technology, Atlanta, Georgia (June 1974).
17. P. Saha, M. Ishii and N. Zuber, An experimental investigation of the thermally induced flow oscillations in two-phase systems, *J. Heat Transfer* **98C**, 616 (1976).
18. N. Zuber, F. W. Staub and G. Bijwaard, Vapor void fraction in subcooled boiling and saturated boiling systems, in *Proceedings of the Third International Heat Transfer Conference*, Vol. 5, p. 24. A.I.Ch.E., New York (1966).
19. N. Zuber and D. E. Dougherty, Liquid metals challenge to the traditional methods of two-phase flow investigations, in *Symposium on Two-Phase Flow Dynamics*, Eindhoven, Vol. 1, p. 1091. EURATOM, Brussels (September 1967).
20. P. G. Kroeger and N. Zuber, An analysis of the effects of various parameters on the average void fractions in subcooled boiling, *Int. J. Heat Mass Transfer* **11**, 211 (1968).
21. S. Y. Ahmad, Axial distribution of bulk temperature and void fraction in a heated channel with inlet subcooling, *J. Heat Transfer* **92C**, 595 (1970).
22. D. S. Lubbers, An investigation of two-phase flows with evaporation, M.S. Thesis, School of Mechanical Engineering, Georgia Institute of Technology, Atlanta, Georgia (June 1974).
23. N. Zuber and J. A. Findlay, Average volumetric concentration in two-phase flow systems, *J. Heat Transfer* **87C**, 453 (1965).
24. M. J. Lighthill and G. B. Whitham, On kinematic waves, *Proc. R. Soc.* **229A**, 281 (1955).
25. G. B. Wallis, *One-Dimensional Two-Phase Flow*, Chapter 6. McGraw-Hill, New York (1969).
26. B. Porter, *Stability Criteria for Linear Dynamical Systems*. Academic Press, New York (1968).
27. E. P. Popov, *The Dynamics of Automatic Control System*. Pergamon Press, Oxford (1962).

ETUDE ANALYTIQUE DES INSTABILITES THERMIQUES D'UN ECOULEMENT BIPHASIQUE AVEC EFFET DU DESEQUILIBRE THERMIQUE

Résumé—On étudie analytiquement le problème des instabilités de l'écoulement induites thermiquement dans un canal avec ébullition. L'effet du déséquilibre thermique entre phases a été pris en compte dans une équation constitutive du débit massique de vapeur générée en considérant l'état énergétique stationnaire. L'équation caractéristique du système est établie en introduisant une petite perturbation en vitesse d'entrée et la stabilité marginale est déterminée en utilisant la méthode *D* de partition. Comparée à la théorie avec équilibre, la théorie du non équilibre prévoit un système plus stable aux faibles nombres de sous-refroidissement et un système plus instable aux grands nombres. Comparée avec les expériences, la théorie présentée ici est en bon accord en ce qui concerne la stabilité marginale aux faibles sous-refroidissement et la fréquence des oscillations. Néanmoins des études ultérieures sont nécessaires pour de meilleures estimations de la stabilité marginale pour les forts sous-refroidissements.

EINE ANALYTISCHE UNTERSUCHUNG DER THERMISCH ANGEREGTEN
INSTABILITÄTEN BEI ZWEIFASENSTRÖMUNG UNTER
BERÜCKSICHTIGUNG DES EINFLUSSES DES THERMISCHEN
NICHT-GLEICHGEWICHTES

Zusammenfassung—Das Problem der thermisch angeregten Strömungsinstabilitäten in einem gleichmäßig beheizten Siedekanal wurde analytisch untersucht. Der Einfluß des thermischen Nicht-Gleichgewichtes zwischen den Phasen wurde berücksichtigt, indem eine Bildungsgleichung für den Massenstrom der Dampfbildung hergeleitet wurde aus stationären Energiebetrachtungen. Die das System charakterisierende Gleichung wurde hergeleitet, indem eine kleine Störung der Eintrittsgeschwindigkeit überlagert wurde. Die Stabilitätsgrenze des Systems wurde bestimmt unter Verwendung der D-Verteilungsmethode. Bei einem Vergleich mit der Gleichgewichtstheorie ergibt die vorliegende Nicht-Gleichgewichtstheorie ein stabileres System bei großer Unterkühlung. Bei einem Vergleich mit dem Experiment zeigt die vorliegende Nicht-Gleichgewichtstheorie gute Übereinstimmung mit den Ergebnissen für die Stabilitätsgrenze des Systems bei kleiner Unterkühlung und mit der Frequenz der Oszillationen. Es müssen jedoch weitere Untersuchungen durchgeführt werden, um die Vorhersage der Stabilitätsgrenze des Systems bei großer Unterkühlung zu verbessern.

АНАЛИТИЧЕСКОЕ ИССЛЕДОВАНИЕ ТЕРМИЧЕСКИ ИНДУЦИРОВАННОЙ
НЕУСТОЙЧИВОСТИ ДВУХФАЗНОГО ТЕЧЕНИЯ, В ТОМ ЧИСЛЕ ЭФФЕКТА
ТЕПЛОВОГО НЕРАВНОВЕСИЯ

Аннотация—Приводится аналитическое решение задачи термически индуцированной неустойчивости течения в равномерно нагретом канале при кипении. Влияние теплового неравновесия между фазами учитывается с помощью определяющего уравнения, выведенного для весовой скорости парообразования по энергии установившегося состояния. Выведено характеристическое уравнение для системы путем введения в скорость небольшого возмущения на входе, а граница устойчивости системы определяется методом разбегания. По предлагаемой теории неравновесного состояния, в противоположность равновесной теории, более устойчива система при небольшом недогреве и менее устойчива при большом недогреве. При сравнении с экспериментом предлагаемая теория неравновесного состояния хорошо согласуется с данными для границы устойчивости системы при небольшом недогреве и небольшой частоте колебаний. Однако для более точного расчета границы устойчивости системы при большом недогреве необходимы дальнейшие исследования.